Cellulose nanocomposites reinforced with bacterial cellulose sheets prepared from pristine and disintegrated pellicle

Alba Santmarti[a], Hanyu Zhang[a], Timo Lappalainen[b], Koon-Yang Lee[a,*]

[a] Department of Aeronautics, Imperial College London, South Kensington Campus, SW7 2AZ, London, UK

[b] VTT Technical Research Centre Finland, Koivurannantie 1, 40101 Jyväskylä, Finland

*Corresponding authors: Email (KYL): koonyang.lee@imperial.ac.uk; Tel: +44 (0)20 7594 5150; Fax: +44 (0)20 7383 2348

Abstract

BC sheets can be prepared in two forms: direct press-drying of the as-synthesised BC pellicle or disintegrating the BC pellicle to create a homogenous BC-in-water suspension prior to producing the BC sheet. We found that BC sheet prepared from direct press-drying of pristine pellicle was more homogeneous due to its better BC network formation and possessed higher specific surface area (46 g m^{-2}), better resin impregnation and mechanical properties compared to its disintegrated pellicle counterpart (21 g m^{-2}). BC-poly(acrylated epoxidised soybean oil) (polyAESO) nanocomposites consisting of BC sheet prepared from pristine pellicle was optically transparent whilst BC-polyAEO nanocomposites consisting of BC sheet prepared from disintegrated pellicle was opaque. Whilst the tensile properties of BC-polyAESO nanocomposites from pristine pellicle were higher, the fracture toughness of BC-polyAESO composite consisting of BC sheet from disintegrated pellicle was better. The lack of resin impregnation in BC-polyAESO from disintegrated pellicle led to a laminated structure, which utilised the fracture toughness of BC sheet effectively.

Keywords

(A) Biocomposite; (B) Fracture toughness; (D) Mechanical testing; bacterial cellulose

1.0 Introduction

Microbially-synthesised cellulose, also known as bacterial cellulose (BC), is a "*jelly-like translucent mass on the surface of the culture fluid*" discovered by Brown more than a century ago [1]. It is synthesised through the fermentation of low molecular weight sugars by cellulose-producing bacteria of the genus *Komagataeibacter* [2]. BC is produced as a pellicle (thick biofilm) consisting of a three-

dimensional network of cellulose nanofibres with a diameter of 50 nm and several micrometres in length [3]. The Young's modulus of a single BC nanofibre is estimated to be 114 GPa [4], exceeding that of glass fibres, which typically possess a Young's modulus of only 70-90 GPa. In terms of potential applications, BC has been explored for wound dressing [5], ultrafiltration membranes for water purification [6], separators for rechargeable Li-ion batteries [7], as well as reinforcement in polymer [8,9].

One of the earlier attempts to utilise BC as reinforcement for polymers was reported by Grunert and Winter [10], whereby the authors reinforced cellulose acetate butyrate (CAB) with BC nanowhiskers produced by sulfuric acid hydrolysis. Whilst the authors did not report the quasi-static mechanical properties of the resulting BC nanowhisker-reinforced CAB composites, their results showed that at a 10 wt.-% loading of BC nanowhiskers, the storage modulus of the BC composites increased by two-fold compared to neat CAB. Gindl and Keckes [11] followed up this concept and produced BC-reinforced CAB composites by solvent exchanging the water in the BC pellicle through ethanol and acetone into CAB dissolved in acetone, followed by solvent removal and compression moulding. At a BC loading of 32 vol.-%, the resulting BC-reinforced CAB composites possessed a tensile modulus and strength of 5.8 GPa and 129 MPa, respectively. Neat CAB was found to possess a tensile modulus and strength of only 1.2 GPa and 26 MPa. This study shows the potential of BC as reinforcement for polymers.

A pre-requisite to produce high performance BC nanocomposites with tensile modulus and strength exceeding that of 4 GPa and 70 MPa, respectively, is to achieve a BC loading of greater than 30 vol.-% [12]. In this context, dried and well-consolidated sheets of BC can be used a precursor to BC-reinforced polymer nanocomposite due to the simplicity in the composite manufacturing process. BC pellicle can be directly press-dried at elevated temperature, consolidating the pristine cellulose nanofibre network as synthesised by the cellulose-producing bacteria and impregnated with a polymer solution[13–15] or a liquid resin or monomer [16–18], followed by crosslinking to produce BC-reinforced polymer nanocomposites with high cellulose loading. Another method to produce dried and well-consolidated sheets of BC is akin to papermaking. BC pellicles can be disintegrated to first create a suspension of BC-in-water with a typical consistency of 0.1 – 0.5 wt.-%, followed by dewatering

through filtration or heat. The filter cake is then press-dried at elevated temperature to produce the BC sheet, which can then be impregnated with a liquid resin [19–21] or laminated with thermoplastics [22–24] to produce BC-reinforced polymer nanocomposites.

BC is grown in a batch process, often using a static culture. As a result, BC sheets from press-dried pristine BC pellicle will have a dimensional and grammage limitations. The dimension of BC pellicle is constrained by the size of the culture vessel whilst the grammage of the BC pellicle is limited by the diffusion of oxygen and nutrients for bacteria growth and hence, BC biosynthesis. These rate limiting steps could be circumvented by producing BC sheets from disintegrated BC pellicles as a suspension of BC-in-water is first created, independent of the dimension or grammage of the starting BC pellicle. This will also allow for the continuous BC sheet production and the grammage of the BC sheet can be specifically tailored, similar to that of a papermaking process. While it is evident that BC sheets, whether if it is made directly from pristine BC pellicle or from disintegrated BC pellicle, could be used to produce high performance BC-reinforced polymer nanocomposites, the differences in the properties and reinforcing efficiency for polymers of the different types of BC sheet have not been reported. In this work, we elucidate the similarities or differences between these two types of BC sheet. The reinforcing ability of both types of BC sheet for poly(acrylated epoxidized soybean oil) (polyAESO) are also discussed in this work.

2. Experimental

2.1 Materials

Formamide (AnalaR NORMAPUR®, purity ≥ 99.7%), ethylene glycol (AnalaR NORMAPUR®, purity ≥ 99.8%), dimethyl sulfoxide (GPR Rectapur®, purity ≥ 100%) and sodium hydroxide pellets (AnalaR NORMAPUR®, purity ≥ 98.5%) were purchased from VWR International Ltd. (Leicestershire, UK). Dimethylformamide (Alfa Aesar, purity ≥ 99%) was purchased from Fisher Scientific Ltd. (Loughborough, UK). Acrylated and epoxidised soybean oil (AESO) (Aldrich, density = 1.04 g cm^{-3}, inhibited with 4000 ppm monomethyl ether hydroquinone) and tert-butyl peroxybenzoate (Luperox® P, Aldrich, purity ≥ 98%) were purchased from Sigma-Aldrich Company Ltd. (Dorset, UK) and used as the thermosetting resin and thermal initiator, respectively. All these chemicals were used without further purification. BC pellicle (30 cm × 30 cm × 1 cm) with a water

content of 98 wt.-% was purchased from a commercial retailer (Vietcoco International Co. Ltd, Ho Chi Minh City, Vietnam).

2.2 Purification of BC pellicle

The purification of BC pellicle in this study was conducted following our previous work [18]. Briefly, BC pellicle (175 g wet weight) was heated to 80 °C under magnetic stirring in 4 L of de-ionised water. To this, NaOH pellets (16 g, 0.4 mol) were added and the BC pellicle was left to stir in this 0.1 N NaOH aqueous solution at 80 °C for 2 h to remove any remaining microorganism or soluble polysaccharides. After this step, the purified BC pellicle was then left to cool to room temperature before rinsing with de-ionised water until a neutral pH was attained. All purified BC pellicles were kept hydrated and stored in a 4 °C fridge prior to subsequent use.

2.3 Preparation of BC sheets

Two types of dried and well-consolidated BC sheet were prepared and studied in this work: (i) BC sheets prepared from pristine, non-disrupted BC nanofibre network as synthesised by the cellulose-producing bacteria and (ii) BC sheets prepared from disintegrated BC pellicles. All the prepared BC sheets possessed a grammage of 65 ± 5 g m^{-2}. To prepare BC sheet directly from the pellicle, the purified BC pellicle (cut to 8 cm × 8 cm) was first gently pressed between two filter papers (Qualitative filter paper 413, VWR International Ltd., Lutterworth, UK) to remove excess moisture on the pellicle surface. This was then followed by a heat consolidation step, whereby the pellicle was sandwiched between two filter papers (Qualitative filter paper 413, VWR International Ltd., Lutterworth, UK) placed in between blotting papers (Grade 3MMCHR, GE Healthcare, Buckinghamshire, UK) and heat-pressed under a weight of 1 t at 120 ºC for 30 min. Prior to preparing BC sheet from disintegrated pellicle, the purified BC pellicle was first cut into 1 cm × 1 cm × 1 cm pieces and disintegrated in water at a consistency of 0.1 wt.-% using a blender (Breville BVL065) for 4 min to obtain a BC-in-water suspension. This suspension was vacuum filtered onto a 125 mm diameter filter paper in a Büchner funnel. The wet BC filter cake was carefully removed and heat-pressed under a weight of 1 t at 120 ºC for 30 min following previously described steps.

2.4 Preparation of BC-reinforced polyAESO nanocomposites

Prior to BC-reinforced polyAESO nanocomposite preparation, AESO was heated to 80 ºC to reduce its viscosity. Luperox® P was then added at a weight ratio of 100:5 and the mixture was de-gassed at a reduced pressure of 100 mbar for 45 min. Once air bubbles were no longer visible, the prepared BC sheet was immersed into the resin and kept at 80 ºC for 1 h under vacuum. The resin-soaked BC sheet was then sandwiched between two nylon 6,6 peel-plies (AeroFilm® PP180, 85 g m^{-2}, Easy Composites Ltd., Staffordshire, UK) placed between two PTFE coated metal plates under a consolidation weight of 2 kg and heat to 110 ºC for 2 h to polymerise the AESO, followed by a post-polymerisation step at 130 ºC for another 2 h. The BC loading fraction in these composites was 50 wt.-%. As a comparison, neat polyAESO was also prepared following the previously described polymerisation steps between two non-stick 125 μm thick polyester release films (Mylar A, Lohmann Adhesive Tape System, Milton Keynes, UK).

2.5 Characterisation of the BC sheets and BC-reinforced polyAESO nanocomposites

2.5.1 β – radiography of BC sheets

In the measurement system, a reusable storage phosphor screen (SPS, BAS IP-MS 2325, Fujifilm Sweden, Stockholm, Sweden) was exposed through the BC sheets with beta radiation. Carbon-14 source with a size of 200 mm × 200 mm × 1 mm (14-C polymer standard source, Nycomed Amersham, Buckinghamshire, U.K.) was used as the source of radiation. The maximum and weighted mean energies of the emitted beta radiation were 156 keV and 49 keV, respectively. A calibration target made of different thicknesses (15-125 μm) of Mylar films (principally polyethylene terephthalate) was attached to the radiation source. Due to similarity of chemical composition, the attenuation of beta particles in Mylar and cellulose should be quite similar [25,26]. The SPS was scanned at 100 μm resolution with a Fuji BAS-1800 II SPS reader (Fujifilm Sweden, Stockholm, Sweden) in order to determine the absorption map of radiation. Those values were then converted into a grammage map.

2.5.2 Porosity of the BC sheets and their respective polyAESO nanocomposites

The true density (ρ_t) of the prepared BC sheets, their respective composites and neat polyAESO was measured using He pycnometry (Accupyc II 1340, Micrometrics Ltd., Dunstable, UK). To determine the envelope density (ρ_e) of the specimens, the thickness was measured using a digital micrometer (Mitutoyo MDC Lite, RS Components Ltd., Northants, UK). With the thickness known, ρ_e was

calculated by dividing the weight of the specimen with its envelope volume. Porosity (*P*) of the BC sheets, their respective composites and neat polyAESO was calculated using:

$$P[\%] = \left(1 - \frac{\rho_e}{\rho_t}\right) \times 100 \quad (1)$$

2.5.3 Specific surface area of the BC sheets

N_2 adsorption/desorption analysis was conducted using a surface area analyser (TriStar 3000, Micrometrics Ltd, Dunstable,UK) to determine the specific surface area of the BC sheets. Prior to the measurement, the samples were purged with N_2 at 120 ºC for 2 h to remove adsorbed water molecules. A sample mass of 70 mg was used in each measurement. The Brunauer−Emmett−Teller (BET) method was used to calculate the surface area of the BC sheets.

2.5.4 Critical surface tension (γ_c) of the BC sheets

The γ_c of the BC sheets was determined from wicking measurements of various test liquids with different surface tensions using the capillary rise technique (Krüss K100 Tensiometer, software version K3.1, Hamburg, Germany). Prior to the measurement, the prepared BC sheets were cut into rectangular specimens with a length of 20 mm and a width of 5 mm. One end of the specimen was fixed onto the tensiometer, which was connected to a microbalance (resolution = 0.01 mg). The reservoir containing the test liquid was moved upwards until the test liquid was in contact with the specimen. At this point, the movement of the reservoir was stopped. This was to ensure that the mass gain of the specimen was only a result of capillarity. The mass gain of the specimen was then measured as a function of time. The obtained data was then analysed using the Washburn equation for single capillary [27]:

$$\gamma_{LV} \cos\theta = \left[\frac{2}{A^2 r}\right]\left[\frac{\eta}{\rho^2}\right]\left[\frac{m^2}{t}\right] \quad (2)$$

where γ_{LV}, η, and ρ are the surface tension, viscosity and density of the test liquid in the reservoir, respectively, whilst m, A, r, θ and t are the mass gain of the specimen during the test, cross-sectional area of the capillary, radius of the capillary, contact angle and time, respectively. However, the radius and area of the capillaries in a well-consolidated BC sheet are not well-defined. Therefore, equation (2) is simplified further by assuming $C = \frac{A^2 r}{2}$, i.e. the geometry of the capillary is constant throughout the measurement [28], resulting in the following equation:

$$C\gamma_{\mathrm{LV}}\cos\theta = \left[\frac{\eta}{\rho^2}\right]\left[\frac{m^2}{t}\right] \quad (3)$$

By plotting the normalised wetting rates $\left[\frac{\eta}{\rho^2}\right]\left[\frac{m^2}{t}\right] = f(\gamma_{\mathrm{LV}})$ of each test liquid, the γ_{c} of BC sheet can be determined from the maxima of the graph. An average of five measurements was taken for each test liquid. The properties of the test liquids used in this study are summarised in Table 1.

2.5.5 Tensile properties of BC sheets and their respective BC-reinforced polyAESO nanocomposites

Tensile test was performed using a micro-tensile tester (Model MT- 200, Deben UK Ltd, Woolpit, UK) equipped with a 200 N load cell. Prior to the test, all samples were cut into rectangular shape test specimens using a Zwick/Roell ZCP 020 manual cutting press (Zwick testing machines ltd, UK). The test specimens had an overall length of 35 mm and a width of 5 mm. The test specimens were secured onto paper testing cards (140 g m^{-2}) using a two-part cold curing epoxy resin (Araldite 2011, Huntsman Advanced Materials, UK) to avoid the clamps of the micro-tensile tester from damaging the ends of the test specimens, potentially leading to earlier onset failure within the gripping zone of the test specimens. The exposed (gauge) length of the rectangular test specimens was 25 mm. Before the test, two points were marked on the surface of the test specimen in the loading direction, which allowed for the strain of the test specimen to be monitored and evaluated based on the movements of these marked points using a non-contact optical extensometer (iMetrum Ltd, Bristol, UK). Tensile test was conducted using a crosshead displacement speed of 0.5 mm min^{-1}, which corresponded to a specimen strain rate of 0.0003 s^{-1}. Average results of 5 test specimens were reported for each sample. All tests were performed at room temperature (22 °C) and at a relative humidity of 40%.

2.5.6 Single-edge notched tension fracture toughness of BC sheets and their respective nanocomposites

The fracture toughness of the BC sheets and the BC-reinforced polyAESO nanocomposites was evaluated from single edge notched tension test. The test specimens possessed a width (w) of 15 mm and a length of 35 mm. An initial crack, a, was introduced in the direction perpendicular to the loading direction at the centre line of the specimen using a sharp scalpel. The single edge notched test specimen was then loaded in tension at a crosshead speed of 0.5 mm min^{-1} using a micro-tensile tester (Model MT- 200, Deben UK Ltd, Woolpit, UK) equipped with a 200 N load cell. The distance between the

grips was set to be 25 mm and a non-contact optical extensometer (iMetrum Ltd., Bristol, UK) was used to monitor the elongation of the test specimen. The initial critical stress intensity factor, K_{IC}, of the BC sheets and their respective polyAESO nanocomposites was calculated from the maximum stress ($\sigma_{\max}$), which corresponded to the propagation of the introduced initial crack, using [29]:

$$K_{\mathrm{Ic}} = Y \times \sigma_{\max}\sqrt{a} \quad (4)$$

where Y is a function related to initial sample geometry, given by the following equation [30]:

$$Y = 1.99 - 0.41 \times \left(\frac{a}{w}\right) + 18.7 \times \left(\frac{a}{w}\right)^2 - 38.38 \times \left(\frac{a}{w}\right)^3 + 53.85 \times \left(\frac{a}{w}\right)^4 \quad (5)$$

The value of a was kept between 3 and 4.5 mm to ensure that the ratio, a/w, was between 0.2 to 0.3 to ensure the validity of equation (5). An average of 5 test specimens were reported for each sample.

2.5.6 Scanning electron microscopy (SEM)

The fracture surface of the single edge notched tension test specimens was investigated using a large chamber scanning electron microscope (S-3700N, Hitachi, Tokyo, Japan). The fractured samples were mounted onto aluminium stubs and Au coated (Agar Auto Sputter Coater, Essex, UK) at 40 mA for 20 s prior to SEM.

3. Results and discussion

3.1 BC network formation of sheets prepared from pristine and disintegrated pellicle

Figure 1 shows the β–radiography of prepared BC sheets. The colour coding refers to the variation in the grammage on the BC sheet. It can be seen from this figure that both types of BC sheet possessed different degrees of inhomogeneity in BC network formation (defined in terms of local variation in BC grammage within a given area). In some regions on the BC sheet, the local BC grammage was found to be as high as 85 g m^{-2}, whilst on other regions, the local BC grammage was as low as 55 g m^{-2}. BC sheet prepared from pristine BC pellicle (Fig. 1a) possessed a smaller degree of inhomogeneity in its BC network formation and this is hypothesised to stem from the uniform biosynthesis of cellulose nanofibers by cellulose-producing bacteria. The high degree of inhomogeneity in BC network formation of the BC sheet prepared from disintegrated BC pellicle (see Fig. 1b) can be attributed to difficulty of blending BC pellicle to produce a homogeneous BC-in-water suspension [31]. As a result, aggregates

or bundles of BC were present in the suspension, leading to the observed poor BC network formation seen in Fig. 1b.

Whilst this poor BC network formation could potentially be resolved using higher energy BC pellicle disintegration or homogenisation process, recent research [32] showed that when BC pellicles were passed through a high energy homogenisation process, such as that of a disk mill, severe damage to the BC was observed. This led to a decrease in the average molecular weight of BC from 819 kDa to only 431 kDa and subsequently the mechanical performance of the resulting BC sheet. Moreover, nanocellulose is a well-known thickening agent. Gelation could occur at cellulose nanofibre concentrations as low as 0.1 wt.-% due to electrostatic forces and the entanglement of cellulose nanofibres [33]. The increase in viscosity reduces the effectiveness of the homogenisation process.

3.2 Surface and bulk properties of BC sheets prepared from pristine and disintegrated BC pellicle

Table 2 summarises the porosity and specific surface area of the prepared BC sheets. Under the same processing condition, both types of BC sheet were found to possess similar porosity of 38%. However, BC sheet prepared from pristine BC pellicle was found to possess higher specific surface area of 46 $m^2 g^{-1}$, whereas its counterpart prepared from disintegrated BC pellicle possessed a specific surface area of only 21 $m^2 g^{-1}$ (see Table 2). He pycnometry showed that both types of BC sheet possessed the same true density, implying that the BC sheets are open porous. As the porosity of both BC sheets was found to be similar, this implied that the loss of surface area of the BC sheet prepared from disintegrated BC pellicle is a direct result of BC aggregation, reducing the surface area.

3.3 Wetting kinetics and critical surface energy of the prepared BC sheets

The thin-layer wicking technique [34] was used to characterise the wetting kinetics and determine the surface energy of the prepared BC sheets. Typical wetting curves are shown in Fig. 2a. The curves exhibited an initial linear behaviour, which corresponded to the absorption of liquid due to capillarity. A plateau was then observed when the capillary forces were balanced by gravity. From the initial slope of the wetting curves, the normalised wetting rates (right hand side of equation 3) can be plotted against the surface tension of the test liquids used (Fig. 2b). The maxima of this plot corresponds to the critical surface energy of the BC sheet, which is defined as the surface tension of an imaginary liquid that will

just wet the BC sheet completely. This is also analogous to the Zisman's solid-vapour critical surface tension [35]. A Gaussian function was used to fit the experimental data in Fig. 2b and the results are summarised in Table 2. The γ_c of both types of BC sheet was found to be similar at 50 mN m^{-1}, indicating that the BC pellicle disintegration process does not alter in the surface energetics of BC. This also implies that the thermodynamic adhesion between the BC sheet and a polymer matrix will be independent of the formation of the BC sheet. It is worth mentioning that liquids with surface tension lower than γ_c will fully wet the BC sheets whilst liquids with surface tension greater than γ_c will only partially wet the BC sheets. Therefore, the surface tension of AESO was also measured as it was used as the monomer in this work. The surface tension of AESO at 80 °C measured with the Krüss K100 tensiometer was found to be 31.1 ± 0.1 mN m^{-1} indicating that AESO will fully wet the BC sheets [36]. The test liquid used in the wetting kinetic measurements of BC sheets was further substituted with AESO heated to 80 °C to study the resin uptake of the prepared BC sheets (see Fig. 2c). Despite both BC sheets possessing similar γ_c and porosity, higher AESO uptake was observed for the BC sheet prepared from pristine BC pellicle compared to its disintegrated BC pellicle counterpart. These results showed that the BC sheet prepared from pristine BC pellicle has smaller capillary (or pore) radius, due to its better BC network formation and less BC aggregation.

3.3 Mechanical properties of the prepared BC sheets

3.3.1 Tensile properties of the BC sheets

The representative stress-strain curves of BC sheets prepared from pristine and disintegrated BC pellicle are shown in Fig. 3a and the tensile properties of these BC sheets are summarised in Table 3. BC sheet made from pristine BC pellicle possessed a higher tensile modulus and strength of 19.6 GPa and 188 MPa, respectively. By comparison, the tensile properties of BC sheet prepared from disintegrated BC pellicle was found to be lower, with a measured tensile modulus of only 13.8 GPa and a tensile strength of 158 MPa. As both types of BC sheet possessed the same porosity, this decrease in tensile properties could be delineated to the presence of BC agglomerates and poor BC network formation of the BC sheet prepared from disintegrated BC pellicle (see Fig. 1). The poor formation of BC sheet from disintegrated pellicle reduced the stress-transfer efficiency between the BC. Similar results were also observed in

conventional handsheets made from pulp fibres, whereby poor formation led to lower tensile properties [37].

Whilst the tensile modulus and strength of BC sheet prepared from pristine BC pellicle was higher, it was more brittle compared to BC sheet prepared from disintegrated BC pellicle. The strain-at-break and the work-of-fracture of BC sheet prepared from pristine BC pellicle was 1.4% and 1.6 MJ m^{-3}, respectively, whilst BC sheet prepared from disintegrated BC pellicle possessed a higher strain-at-break of 3% and work-of-fracture of 3.3 MJ m^{-3}. The lower ductility of BC sheet made from pristine BC could be due to its more uniform BC network formation, which is hypothesised to possess more physical crosslinking points between the nanofibres. As a result, the nanofibres in the BC sheet do not realign easily when they are subjected to a tensile force, leading to tensile failure with little plastic deformation. Due to the poorer BC network formation in the BC sheet prepared from disintegrated BC pellicle, regions with lower grammage, which has less degree of hornification, could potentially deform more and absorb more energy under tensile loading, whilst regions with higher grammage provided structural support to the BC sheet.

3.3.2 Single-edge notched tension (SENT) fracture toughness of the BC sheets

Figure 3b presents the mechanical response of single-edge notched tension specimens of BC sheet. The initial linear part of the curve corresponded to an elastic response. Once maximum load was reached, the crack on the single-edge notched tension specimen propagated. It can be seen from this figure that BC sheet produced from disintegrated BC pellicle failed at higher displacement compared to BC sheet produced from pristine pellicle. Furthermore, plastic deformation can be observed for BC sheet from disintegrated pellicle. This is due to the higher strain-at-failure of the BC sheet made from disintegrated pellicle compared to pristine BC pellicle. Moreover, the poor BC network formation of BC sheet prepared from disintegrated pellicle further provided additional energy absorbing mechanism [31]. When the crack propagated, the crack front encountered inhomogeneity in the form of agglomerated BC, which led to crack diversion. This is further confirmed with SEM imagines of the fracture surfaces of the single-edge notched tension specimens (see Fig. 4). Two different fracture morphologies can be

observed. The SENT fracture surface of BC sheet from pristine pellicle was smooth whilst significant defibrillation can be observed for BC sheet prepared from disintegrated pellicle.

The initial critical stress intensity factor (K_{IC}) of the BC sheets are also summarised in Table 3. BC sheet prepared from pristine BC pellicle possessed a K_{IC} value of 11.9 MPa $m^{1/2}$. When the BC pellicle was disintegrated prior to producing a BC sheet, the resulting BC sheet possessed a lower K_{IC} of 9.7 MPa $m^{1/2}$ [38]. These results corroborated the tensile strength of the BC sheets, whereby the higher the tensile strength, the higher the fracture toughness of the resulting BC sheet. This is because the mechanism behind both the crack opening of the single-edge notch tension specimen and the failure of the BC specimen under uniaxial tensile loading are similar, involving nanofibre-nanofibre debonding and fracture. It is also worth mentioning that the K_{IC} values for BC sheets are found to be higher than that of single AS4 carbon, Kevlar and S-glass fibres, measured to be 2.12 MPa $m^{0.5}$, 1.08 MPa $m^{0.5}$ and 6.63 MPa $m^{0.5}$, respectively, using the same single-edge notched tension test.

3.4 Visual appearance of the resulting BC-reinforced polyAESO composites

When light travels through two materials with different refractive indices (RI), light diffracts at the interface. The transparency of a composite material depends on the loading fraction and the dimension of the dispersed phase, as well as RI mismatch between the continuous phase and the dispersed phase [39]. The smaller the volume fraction and dimension of the dispersed phase, as well as the smaller the RI mismatch between the two phases, the more transparent the composite will be. Cellulose fibres have a RI of 1.618 along the fibre axis and 1.544 in the transverse direction [40]. Epoxidized soybean oil, on the other hand, possessed a RI of 1.470 - 1.475 [41]. Despite this RI mismatch, BC-polyAESO nanocomposites consisting of BC sheet from pristine BC pellicle was still transparent (see Fig. 5). However, BC-polyAESO nanocomposites consisting of BC sheet from disintegrated BC pellicle was found to be opaque. This stems from the differences in BC network formation of the two types of BC sheet. The presence of significant agglomerations in the BC sheet prepared from disintegrated BC pellicle increased the effective size of BC when interacting with light, as well as reduced the level of resin impregnation (see next section). Both of these factors led to significant light scattering and loss of transparency in the resulting BC-polyAESO nanocomposites consisting of BC sheet prepared from disintegrated pellicle.

3.5 Mechanical properties of the prepared BC-reinforced polyAESO nanocomposites

3.5.1 Tensile properties of the BC-reinforced polyAESO nanocomposites

The representative tensile stress-strain curves of neat polyAESO and BC-reinforced polyAESO nanocomposites are shown in Fig. 6a and Table 4 summarises the mechanical properties of neat polyAESO and both BC-reinforced polyAESO nanocomposites. At similar BC loading fraction of 50 wt.-%, BC nanocomposite reinforced with BC sheet made from pristine pellicle possessed a tensile modulus of 8.6 GPa and a tensile strength of 95 MPa. In comparison, the tensile modulus and strength of the BC nanocomposite reinforced with BC sheet made from disintegrated BC pellicle were found to be 5.7 GPa and 68 MPa, respectively. This is due to the higher porosity of BC nanocomposites reinforced with BC sheet from disintegrated BC pellicle (see Table 4). BC sheet from pristine pellicle was also found to produce composites that were more brittle. BC-reinforced polyAESO nanocomposites reinforced with BC sheet from pristine pellicle possessed lower strain-at-break of 1.8%, compared to 3.2% for nanocomposites reinforced with BC sheet from disintegrated pellicle. This can be attributed to the higher strain-at-break of the BC sheet made from disintegrated BC pellicle.

An interesting observation from Table 4 is that even though the manufactured BC nanocomposites possess similar BC loading, their porosities differ significantly, considering that the starting porosity of both types of BC sheet were similar (see Table 2). We therefore estimated the theoretical porosity ($P_{\text{theoretical}}$) of the nanocomposites using the following equation [23]:

$$P_{\text{theoretical}} = 1 - \frac{\rho_{\text{BC sheet}}}{\rho_{\text{f}}} \left[\frac{(1-w_{\text{f}})\rho_{\text{f}}+w_{\text{f}}\rho_{\text{m}}}{(1-w_{\text{f}})\rho_{\text{BC sheet}}+w_{\text{f}}\rho_{\text{m}}}\right] \quad (6)$$

whereby $\rho_{\text{BC sheet}}$, ρ_{f}, w_{f} and ρ_{m} correspond to the envelope density of the reinforcing BC sheet (see Table 2), the true density of BC (see Table 2), the weight fraction of BC in the nanocomposite and the true density of neat polyAESO, respectively. This equation assumes that BC sheets are incompressible and impermeable to the polymer matrix. Following these assumptions, the $P_{\text{theoretical}}$ of BC nanocomposites based on the attributes of the BC sheets prepared in this work was estimated to be 20%. This value is consistent with BC composites reinforced with BC sheet prepared from disintegrated BC pellicle, suggesting that AESO did not fully impregnate this BC sheet. Instead, the resin mainly laminated the surface of the BC sheet only (see Fig. 7 for the fracture surface of this BC nanocomposite).

The porosity of BC-reinforced polyAESO nanocomposites reinforced with BC sheet from pristine pellicle, on the other hand, was found to possess lower porosity than $P_{\text{theoretical}}$, suggesting higher level of resin impregnation. These results are in concordance with the results from the wetting kinetics of BC sheets by hot AESO resin (see Fig. 2c), whereby BC sheet prepared from pristine pellicle exhibited a higher resin uptake due to capillarity compared to BC sheet made from disintegrated pellicle, as well as the transparency of this BC nanocomposite (see Fig. 5).

3.5.2 Single-edge notched tension (SENT) fracture toughness of the BC-reinforced polyAESO nanocomposites

The mechanical response of the single edge-notched tension polyAESO and BC-reinforced polyAESO nanocomposites test specimens are plotted in Fig. 6b. PolyAESO composites reinforced with BC sheets have a higher fracture toughness than neat polyAESO of only K_{IC} = 0.2 MPa $m^{1/2}$ (see Table 4). However, the type of reinforcing BC sheets employed affects the K_{IC} of the BC nanocomposites; composites reinforced with BC sheet prepared from pristine BC pellicle possessed lower K_{IC} value (2.2 MPa $m^{1/2}$) compared to composites reinforced with BC sheet prepared from disintegrated BC pellicle (3.1 MPa $m^{1/2}$). The higher K_{IC} value of BC-polyAESO composite (disintegrated BC pellicle) could be due to the poor resin impregnation. This poor resin impregnation led to a laminated composite architecture (see Fig. 7). Due to this, the crack propagated through both the polyAESO resin and the BC sheet, fully utilising the fracture resistance of BC sheet from disintegrated BC pellicle. PolyAESO-BC sheet (pristine BC pellicle) composite, on the other hand, possessed a higher level of resin impregnation. Since crack will propagate through the path of least resistance, it is postulated that the crack propagated through the resin of the nanocomposites, which included the resin rich region on the surface of the BC sheet, as well as the resin within the BC sheet. This is further confirmed by the fractographic analysis of the SENT fracture toughness test specimens (see Fig. 7). The fracture surface of polyAESO-BC (pristine pellicle) composites possessed a clean fracture surface and does not exhibit any BC sheet defibrillation (see Fig.5c). Thus, the failure was mainly dominated by the properties of the polyAESO matrix. In Fig.5d, we can observe significant BC sheet defibrillation, as well as ribbons and scarps on the polyAESO matrix, indicating that the specimen failed in a brittle fashion [42]. The

BC sheet in BC-polyAESO (disintegrated pellicle) still exhibits some defibrillation compared to BC-polyAESO (pristine pellicle) due to the lack of resin between the fibres. Therefore, the fracture is mostly BC sheet dominated.

4. Conclusions

Two types of BC sheets were compared in this work: (i) BC sheet prepared from pristine pellicle and (ii) BC sheet prepared from disintegrated pellicle. It was found that BC sheet prepared from pristine pellicle has better BC network formation compared to its disintegrated pellicle counterpart. This is due to difficulties in disrupting the three-dimensional BC nanofibre network synthesised by cellulose-producing bacteria. Consequently, BC sheet prepared from pristine pellicle possessed high specific surface area of 46 g m^{-2}, compared to BC sheet prepared from disintegrated pellicle, which was found to possess a specific surface area of only 21 g m^{-2}. BC sheet prepared from pristine pellicle was also found to possess higher tensile properties and fracture toughness compared to its disintegrated pellicle counterpart. We attributed to the existence of more physical crosslinking points between the BC nanofibres in BC sheet prepared from pristine pellicle. Better fibre-fibre bonding increased the mechanical properties of the resulting BC sheet due to better stress transfer. However, it also reduced its ability to deform plastically, leading to lower work of fracture of the BC sheet prepared from pristine pellicle compared to its disintegrated pellicle counterpart. Whilst wetting kinetic study also showed no significant difference in the critical surface tensions of both types of BC sheet (~50 mN m^{-1}), polyAESO nanocomposites reinforced with BC sheet prepared from pristine pellicle possessed higher tensile modulus and strength at the same BC loading compared to polyAESO composites prepared from disintegrated pellicle. This is due to the higher tensile properties, as well as better resin impregnation of the BC sheet prepared from pristine pellicle. The latter also led to highly transparent polyAESO composites whilst composites reinforced with BC sheet prepared from disintegrated pellicle was found to be opaque. Nevertheless, the better resin impregnation of the BC sheet prepared from pristine pellicle also led to poorer fracture toughness and strain-at-failure of the BC-polyAESO. This is because when there is no resin in between the fibrous network, the fracture resistance behaviour is dominated by the BC sheet performance. In order for the crack to propagate, it needs to overcome fibre-fibre bonds through defibrillation. When the resin impregnated the BC sheet well, the crack propagates through the

path of least resistance, which is the polyAESO between the BC fibres. Our results suggest there is a trade-off between BC sheet from pristine and disintegrated pellicles, particularly for composite applications.

Acknowledgements

The authors would like to thank the UK Engineering and Physical Sciences Research Council (EP/N026489/1) for funding this work. We would also like to acknowledge the financial support from the Department of Aeronautics Imperial College London for funding AS.

References

[1] Brown J. On an acetic ferment which forms cellulose. J Chem Soc, Trans 1886;49:432–9.
[2] Florea M, Hagemann H, Santosa G, Abbott J, Micklem CN, Spencer-Milnes X, et al. Engineering control of bacterial cellulose production using a genetic toolkit and a new cellulose-producing strain. Proc Natl Acad Sci U S A 2016;113:E3431-40. doi:10.1073/pnas.1522985113.
[3] Lee KY, Buldum, 1 K. Y. Lee, G. Buldum, A. Mantalaris and A. Bismarck, Macromol. Biosci., 2014, 14 10–32.Gizem, Mantalaris A, Bismarck A. More than meets the eye in bacterial cellulose: Biosynthesis, bioprocessing, and applications in advanced fiber composites. Macromol Biosci 2014;14:10–32. doi:10.1002/mabi.201300298.
[4] Hsieh Y-C, Yano H, Nogi M, Eichhorn SJ. An estimation of the Young's modulus of bacterial cellulose filaments. Cellulose 2008;15:507–13. doi:10.1007/s10570-008-9206-8.
[5] Portela R, Leal CR, Almeida PL, Sobral RG. Bacterial cellulose: a versatile biopolymer for wound dressing applications. Microb Biotechnol 2019;12:586–610. doi:10.1111/1751-7915.13392.
[6] Mautner A, Lee K-Y, Tammelin T, Mathew AP, Nedoma AJ, Li K, et al. Cellulose nanopapers as tight aqueous ultra-filtration membranes. React Funct Polym 2015;86:209–14. doi:10.1016/j.reactfunctpolym.2014.09.014.
[7] Gwon H, Park K, Chung S-C, Kim R-H, Kang JK, Ji SM, et al. A safe and sustainable bacterial cellulose nanofiber separator for lithium rechargeable batteries. Proc Natl Acad Sci 2019:201905527. doi:10.1073/PNAS.1905527116.
[8] Qiu K, Netravali AN. A Review of Fabrication and Applications of Bacterial Cellulose Based Nanocomposites. Polym Rev 2014;54:598–626. doi:10.1080/15583724.2014.896018.
[9] Shah N, Ul-Islam M, Khattak WA, Park JK. Overview of bacterial cellulose composites: A multipurpose advanced material. Carbohydr Polym 2013;98:1585–98. doi:10.1016/j.carbpol.2013.08.018.
[10] Grunert M, Winter WT. Nanocomposites of cellulose acetate butyrate reinforced with cellulose nanocrystals. J Polym Environ 2002;10:27–30. doi:10.1023/A:1021065905986.
[11] Gindl W, Keckes J. Tensile properties of cellulose acetate butyrate composites reinforced with bacterial cellulose. Compos Sci Technol 2004;64:2407–13. doi:10.1016/j.compscitech.2004.05.001.
[12] Lee K-Y, Aitomäki Y, Berglund LA, Oksman K, Bismarck A. On the use of nanocellulose as reinforcement in polymer matrix composites. Compos Sci Technol 2014;105:15–27. doi:10.1016/j.compscitech.2014.08.032.
[13] Pinto ERP, Barud HS, Silva RR, Palmieri M, Polito WL, Calil VL, et al. Transparent composites prepared from bacterial cellulose and castor oil based polyurethane as substrates for flexible OLEDs. J Mater Chem C 2015;3:11581–8. doi:10.1039/C5TC02359A.
[14] Gea S, Bilotti E, Reynolds CT, Soykeabkeaw N, Peijs T. Bacterial cellulose-poly(vinyl alcohol) nanocomposites prepared by an in-situ process. Mater Lett 2010;64:901–4. doi:10.1016/j.matlet.2010.01.042.

[15] Nakagaito AN, Iwamoto S, Yano H. Bacterial cellulose: The ultimate nano-scalar cellulose morphology for the production of high-strength composites. Appl Phys A Mater Sci Process 2005;80:93–7. doi:10.1007/s00339-004-2932-3.
[16] Nogi M, Yano H. Transparent nanocomposites based on cellulose produced by bacteria offer potential innovation in the electronics device industry. Adv Mater 2008;20:1849–52. doi:10.1002/adma.200702559.
[17] Yano H, Sugiyama J, Nakagaito AN, Nogi M, Matsuura T, Hikita M, et al. Optically Transparent Composites Reinforced with Networks of Bacterial Nanofibers. Adv Mater 2005;17:153–5. doi:10.1002/adma.200400597.
[18] Santmarti A, Teh JW, Lee K-Y. Transparent Poly(methyl methacrylate) Composites Based on Bacterial Cellulose Nanofiber Networks with Improved Fracture Resistance and Impact Strength. ACS Omega 2019;4:9896–903. doi:10.1021/acsomega.9b00388.
[19] Lee KY, Tammelin T, Schulfter K, Kiiskinen H, Samela J, Bismarck A. High performance cellulose nanocomposites: Comparing the reinforcing ability of bacterial cellulose and nanofibrillated cellulose. ACS Appl Mater Interfaces 2012;4:4078–86. doi:10.1021/am300852a.
[20] Ummartyotin S, Juntaro J, Sain M, Manuspiya H. Development of transparent bacterial cellulose nanocomposite film as substrate for flexible organic light emitting diode (OLED) display. Ind Crops Prod 2012;35:92–7. doi:10.1016/j.indcrop.2011.06.025.
[21] Juntaro J, Ummartyotin S, Sain M, Manuspiya H. Bacterial cellulose reinforced polyurethane-based resin nanocomposite: A study of how ethanol and processing pressure affect physical, mechanical and dielectric properties. Carbohydr Polym 2012;87:2464–9. doi:10.1016/j.carbpol.2011.11.020.
[22] Hervy M, Bock F, Lee KY. Thinner and better: (Ultra-)low grammage bacterial cellulose nanopaper-reinforced polylactide composite laminates. Compos Sci Technol 2018;167:126–33. doi:10.1016/j.compscitech.2018.07.027.
[23] Hervy M, Blaker JJ, Braz AL, Lee KY. Mechanical response of multi-layer bacterial cellulose nanopaper reinforced polylactide laminated composites. Compos Part A Appl Sci Manuf 2018;107:155–63. doi:10.1016/j.compositesa.2017.12.025.
[24] Montrikittiphant T, Tang M, Lee K-Y, Williams CK, Bismarck A. Bacterial cellulose nanopaper as reinforcement for polylactide composites: renewable thermoplastic NanoPaPreg. Macromol Rapid Commun 2014;35:1640–5. doi:10.1002/marc.201400181.
[25] Keller DS, Pawlak JJ. β -Radiographic Imaging of Paper Formation Using Storage Phosphor Screens. J Pulp Pap Sci 2001;27:117–23.
[26] Tomimasu H, Luner P, Hanna R. Rapid Imaging of Mass Distribution in Paper by Electrons. Fund. Papermaking 1: Mech. Engineering Pub. Ltd.: London; 1989.
[27] Szekely J, Neumann AW, Chuang YK. The rate of capillary penetration and the applicability of the washburn equation. J Colloid Interface Sci 1971;35:273–8. doi:10.1016/0021-9797(71)90120-2.
[28] Grundke K, Bogumil T, Gietzelt T, Jacobasch H-J, Kwok DY, Neumann AW. Wetting measurements on smooth, rough and porous solid surfaces. In: Jacobasch H-J, editor. Interfaces, Surfactants Colloids Eng., Darmstadt: Steinkopff; 1996, p. 58–68. doi:10.1007/BFb0114445.
[29] F Brown Jr. W, E Srawley J. Plane strain crack toughness testing of high strength metallic materials. Philadelphia: American society for testing and materials; 1966.
[30] Kinloch AJ, Young RJ. Fracture behaviour of polymers. London and New York: Applied Science Publishers; 1983.
[31] Hervy M, Santmarti A, Lahtinen P, Tammelin T, Lee K-Y. Sample geometry dependency on the measured tensile properties of cellulose nanopapers. Mater Des 2017;121:421–9. doi:10.1016/j.matdes.2017.02.081.
[32] Mautner A, Mayer F, Hervy M, Lee KY, Bismarck A. Better together: Synergy in nanocellulose blends. Philos Trans R Soc A Math Phys Eng Sci 2018;376. doi:10.1098/rsta.2017.0043.
[33] Mendoza L, Batchelor W, Tabor RF, Garnier G. Gelation mechanism of cellulose nanofibre gels: A colloids and interfacial perspective. J Colloid Interface Sci 2018;509:39–46.

doi:10.1016/j.jcis.2017.08.101.
[34] Chibowski E, Holysz L. Use of the Washburn equation for surface free energy determination. Langmuir 1992;8:710–6. doi:10.1021/la00038a066.
[35] Tröger J, Lunkwitz K, Grundke K, Bürger W. Determination of the surface tension of microporous membranes using wetting kinetics measurements. Colloids Surfaces A Physicochem Eng Asp 1998;134:299–304. doi:10.1016/S0927-7757(97)00158-1.
[36] Aranberri-Askargorta I, Lampke T, Bismarck A. Wetting behavior of flax fibers as reinforcement for polypropylene. J Colloid Interface Sci 2003;263:580–9. doi:10.1016/S0021-9797(03)00294-7.
[37] Nazhad MM, Harris EJ, Dodson CTJ, Kerekes RJ. The influence of formation on tensile strength of paper made from mechanical pulps. Tappi Papermak Conf Trade Fair 2000;1:141–6.
[38] Herráez M, Fernández A, Lopes CS, González C. Strength and toughness of structural fibres for composite material reinforcement. Philos Trans R Soc A Math Phys Eng Sci 2016;374.
[39] Dunlap, P. N, Howe SE. Design of Particulate Composites for Optical Applications. Polym Compos 1991;12:39–47.
[40] Bandrup J, Immergut EH, Grulke EA, editors. Polymer Handbook. 4th ed. New York, USA: Wiley; 1999.
[41] Retegi A, Algar I, Martin L, Altuna F, Stefani P, Zuluaga R, et al. Sustainable optically transparent composites based on epoxidized soy-bean oil (ESO) matrix and high contents of bacterial cellulose (BC). Cellulose 2012;19:103–9. doi:10.1007/s10570-011-9598-8.
[42] Greenhalgh E. Failure analysis and fractography of polymer composites. Cambridge, UK: Woodhead Publishing Limited; 2009.

List of tables

Table 1: Properties of the test liquids used for wetting measurements. Values obtained from Krüss K100 software version 3.1.

Test liquid	γ_{lv} (mN m^{-1})	η (mPa s)	ρ (g cm^{-3})
Dimethylformamide	37.1	0.92	0.994
Dimethyl sulfoxide	44	2.14	1.104
Ethylene glycol	47.7	16.1	1.11
Ethylene glycol/Water (80:20 wt/wt)	52.2	11.44	1.097
Ethylene glycol/Water (60:40 wt/wt)	55.9	5.69	1.085
Formamide	58.2	3.812	1.133
Ethylene glycol/water (20:80 wt/wt)	64.8	1.331	1.109
Water	72.8	1.002	0.998

Table 2: A summary of the true density (ρ), bulk density (ρ_e), porosity (P), BET surface area (A_s) and critical surface tension (γ_c) of the prepare BC sheets.

BC sheet	ρ_e (g cm^{-3})	ρ (g cm^{-3})	P (%)	A_s (m^2 g^{-1})	γ_c (mN m^{-1})
From pristine BC pellicle	1.60 ± 0.01	0.99 ± 0.01	38 ± 1	46 ± 5	50.6 ± 0.6
From disintegrated BC pellicle	1.61 ± 0.01	1.00 ± 0.02	37 ± 1	21 ± 1	49.9 ± 0.2

Table 3: Mechnical properties of the prepared BC sheets.E Tensile properties, toughness and stress. E, σ, ε, WOF and K_{IC} correpond to the tensile modulus, tensile strength, tensile strain-at-break, work of fracture and critical initial stress intensity factor, respectively.

BC sheet	E (GPa)	σ (MPa)	ε (%)	WOF (MJ m^{-3})	K_{IC} (MPa m$^{1/2}$)
Pristine BC pellicle	19.6 ± 0.3	188 ± 9	1.4 ± 0.1	1.6 ± 0.2	11.9 ± 1.4
Disintegrated BC pellicle	13.8 ± 1.2	158 ± 13	3.0 ± 0.4	3.3 ± 0.4	9.7 ± 0.2

Table 4: The envelope density (ρ_e), porosity (P), BC weight fraction (w_{BC}), tensile modulus (E), tensile strength (σ), tensile strain-at-break (ε), work of fracture (WOF) and critical initial stress intensity factor (K_{IC}) of neat polyAESO and polyAESO-BC composites.

Sample	ρ_e (g cm^{-3})	$P^{\dagger}$ (%)	w_{BC} (%)	E (GPa)	σ (MPa)	ε (%)	WOF (MJ m^{-3})	K_{IC} (MPa m$^{1/2}$)
Neat PolyAESO	1.16 ± 0.01	0	0	0.1 ± 0.1	5 ± 1	8.0 ± 1.0	0.2 ± 0.1	0.2 ± 0.1
BC-reinforced polyAESO nanocomposites								
Pristine pellicle	1.24 ± 0.07	7 ± 5	49 ± 1	8.6 ± 0.7	95 ± 9	1.8 ± 0.3	1.0 ± 0.2	2.2 ± 0.1
Disintegrated pellicle	1.02 ± 0.09	24 ± 7	48 ± 1	5.7 ± 0.3	68 ± 9	3.2 ± 0.6	1.4 ± 0.4	3.1 ± 0.1

†The true density of neat polyAESO and BC-reinforced polyAESO nanocomposites were measured to be 1.16 ± 0.01 g cm^{-3} and 1.34 ± 0.01 g cm^{-3}, respectively.

List of figures

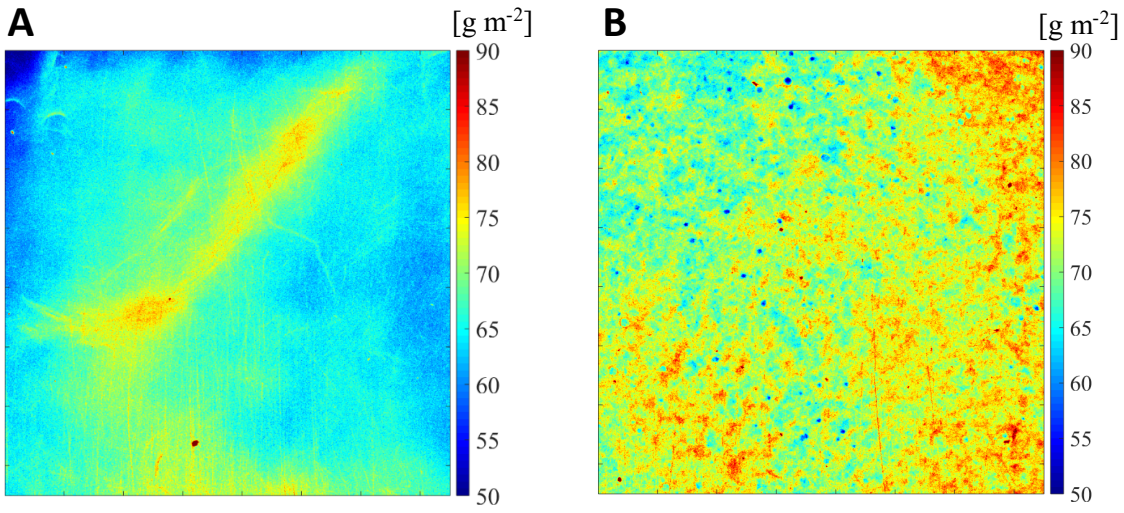

Fig. 1. β-radiography of the prepared BC sheets. The scan area was 75 mm × 75 mm. (A) BC sheet prepared from pristine pellicle and (B) BC sheet prepared from disintegrated pellicle.

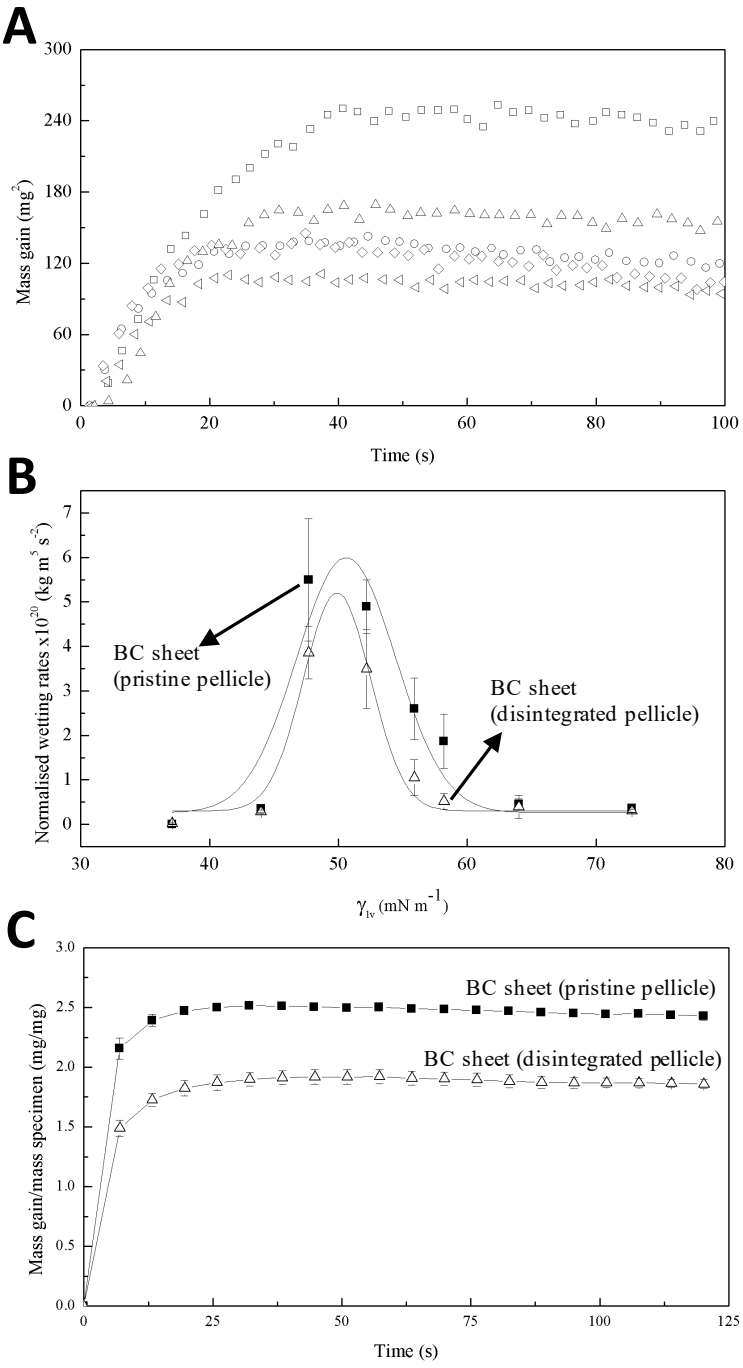

Fig. 2. (a) Exemplar wetting curve. This BC sheet sample was prepared from pristine BC pellicle and the test liquid used was formamide, (b) normalised wetting curves of the BC sheets as a function of the surface tension of the test liquids tabulated in Table 1 and (c) wetting curves of the BC sheets by acrylated epoxidised soybean oil (AESO) at 80 °C.

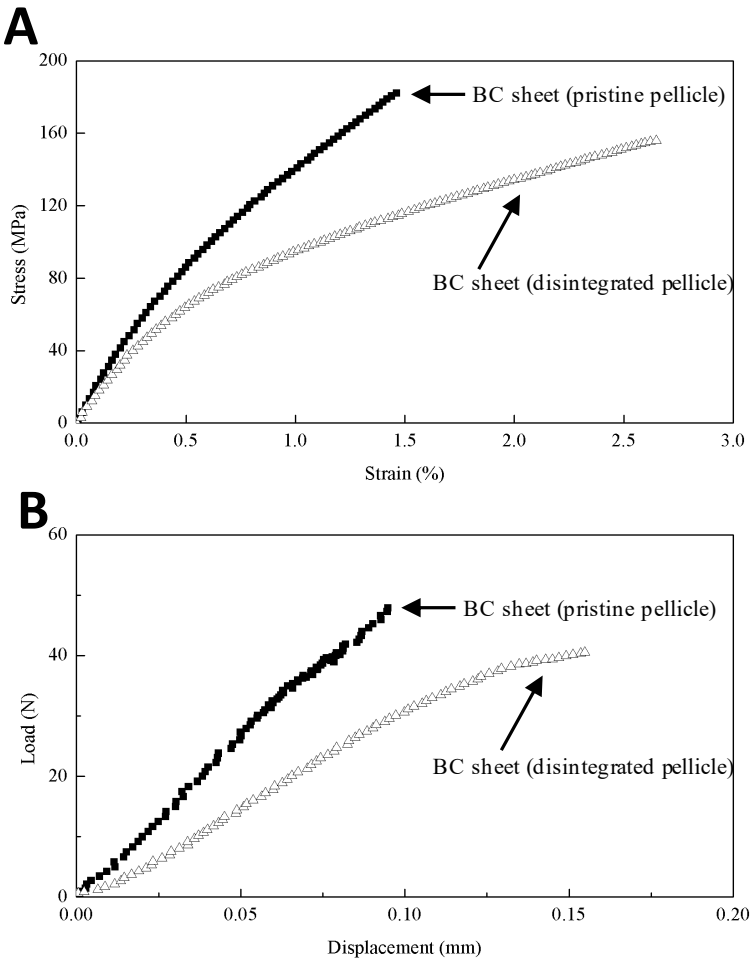

Fig. 3. Typical (a) tensile stress-strain curves and (b) single-edge notched tension load-displacement curves of the prepared BC sheets.

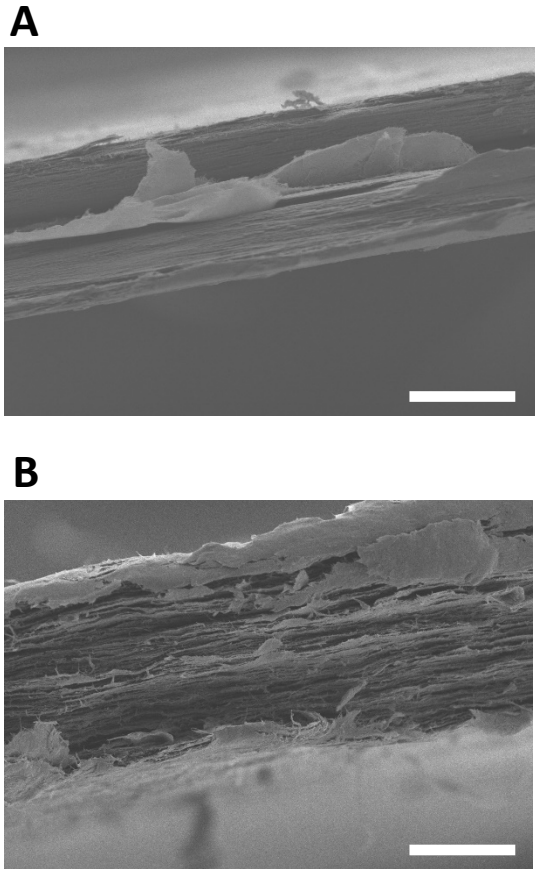

Fig. 4. Fracture surface of BC sheets from single-edge notched tension test. (a) Pristine BC pellicle and (b) disintegrated BC pellicle. Scale bar = 25 µm.

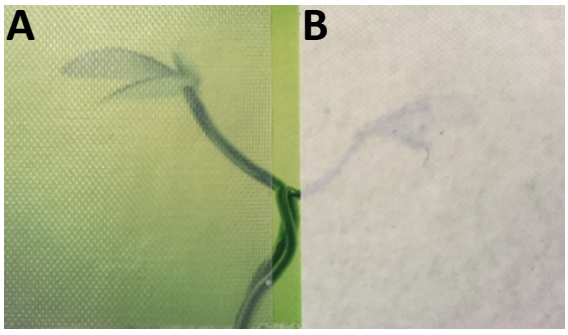

Fig. 5. Visual apperance of BC-polyAESO nanocomposites reinforced with BC sheet prepared from (a) pristine BC pellicle and (b) disintegrated BC pellicle

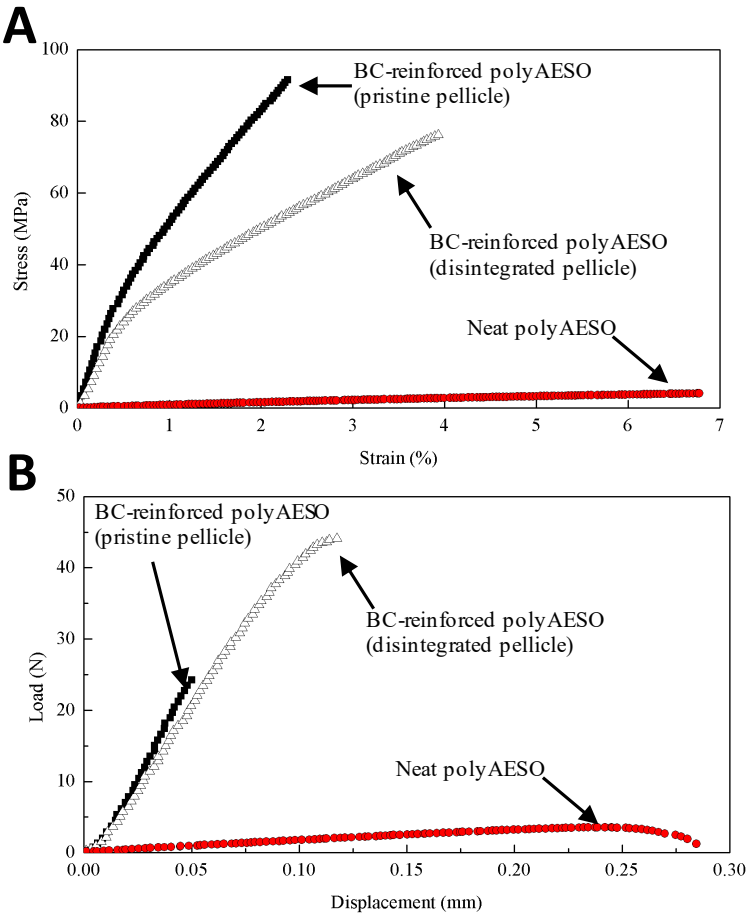

Fig. 6. Typical (a) tensile stress-strain curves and (b) single-edge notched tension load-displacement curves of the prepared BC-reinforced polyAESO composites.

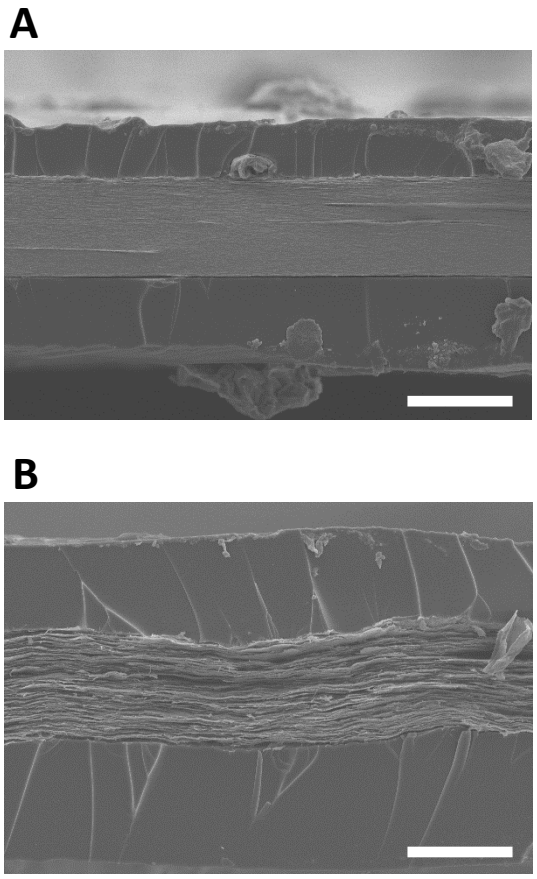

Fig. 7. Fracture surface of BC-reinforced polyAESO nanocomposites from single-edge notched tension test. (a) Composites reinforced with pristine BC pellicle and (b) composites reinforced with disintegrated BC pellicle. Scale bar = 50 µm.